Astron. Astrophys. 202, 267–274 (1988)

ASTRONOMY
AND
ASTROPHYSICS

Radio emission of coronal shock waves

A. O. Benz [1] **and G. Thejappa** [2]

[1] Institute of Astronomy, ETH, Zürich, CH-8092 Zürich, Switzerland
[2] Indian Institute for Astrophysics, Bangalore, India

Received January 14, accepted March 16, 1988

Summary. The "backbone" emission of shock initiated coronal (metric) type II solar radio bursts is considered. The source has extremely narrow bandwidth and appears to be stationary in relation to the shock. The increasingly complete understanding of the phenomena associated with the Earth's bow shock is tapped for suggestions on the responsible particles, their energies and the emission mechanism of radio waves. We propose that the radiation originates from electrons and ions of a few keV energy, the dominant populations of accelerated particles upstream of the bow shock. These particles may locally form velocity distribution that are unstable towards growing electrostatic waves (Z-mode, ion-acoustic and/or lower hybrid waves). The "backbone" source seems to require an exciter that is different from the classical type III producing beam. We suggest a shifted ring distribution (the result of fast Fermi acceleration). Ion beams may excite ion-acoustic and lower-hybrid waves and provide low-frequency turbulence. A model is developed which can explain the major observed features by wave-wave coupling between electron plasma waves themselves and with ion waves. Observational tests at interplanetary and bow shock waves are proposed.

Key words: collisionless shock waves – particle acceleration – type II solar radio bursts

1. Introduction

Accelerated particles at the Earth's bow shock and, in lesser detail, also at interplanetary shocks have been extensively observed by in situ spacecraft. Resolution of small scale structure has recently led to considerable progress in the understanding of the physics of collisionless shocks. On the other hand, a large body of remote observations of flare initiated coronal shocks has been compiled in white light and radio waves (metric type II bursts), but the problems of coronal particle acceleration and radio emission are far from being settled. This work is based on the assumption that despite the different shock parameters the basic physics of these collisionless shocks is essentially the same. Given the present knowledge on the nearly collisionless shocks and recent high resolution metric radio observations, we propose here a new emission process for metric type II bursts.

Coronal (metric) type II events have been observed for more than three decades. The subject has most recently been reviewed by Nelson and Melrose (1985) and Simnett (1986). Figure 1 shows an example of high resolution observations made by the digital spectrometer IKARUS at ETH Zurich (Perrenoud, 1982). We consider the following observational points essential for a possible emission mechanism:

1) Type II events consist of two components: a spiky, narrow band drifting slowly to lower frequency (metaphorically termed "backbone") and rapidly drifting, broad-band structures shooting out of the backbone to lower and higher frequency, called "herringbones". The two components can easily be distinguished in a spectrogramme (cf. Fig. 1, bottom) and are obviously different in their intrinsic time scale and bandwidth. Roberts (1959) reported evidence of "herringbone" structure in 20% of his set of metric type II events, but none has yet been observed in interplanetary shocks. "Herringbones" have a slightly, but consistently higher degree of circular polarization than the "backbone". Note in Fig. 1 that patches in the "backbone" have halfpower bandwidths of only 2–3% of the emission frequency. Single "herringbones" resemble type III bursts and are generally interpreted as signatures of a beam of energetic particles accelerated near the source of the "backbone" (i.e. escaping from the shock). It is widely accepted that the "herringbone" emission is due to Langmuir waves excited by the gentle-bump-instability similar to type III bursts. These electrostatic waves scatter off ion density fluctuations and/or low frequency ion waves to radiate in the ordinary mode at the local plasma frequency. Additionally, they also are known to interact with Langmuir waves propagating in opposite direction, giving rise to emission at the harmonic.

2) Here we concentrate on the unknown emission mechanism of the "backbone". Its small bandwidth seems to exclude interpretations by a type III-like exciter, as attempted by several previous authors. Assuming that the bandwidth is fully determined by inhomogeneity (an upper limit), the source diameter is less than a few percent of the density scale height, or about 1000 km in the undisturbed corona (but less if the source is more inhomogeneous). The source seems to be quasi-stationary in relation to the shock. Such a small size is far below expectation of conventional models for type III-like exciters. It is also more than an order of magnitude smaller than the region of beam excited Langmuir waves at the bow shock (Anderson et al., 1981, see below). This source size and the observed flux lead to a brightness temperature ot the "backbone" structures in Fig. 1 of $\gtrsim 5\ 10^{12}$ K.

3) Despite the obvious difference of the two components there are also striking similarities. The two components are always found to have the same sense of circular polarization (cf. Nelson

Send offprint requests to: A.O. Benz

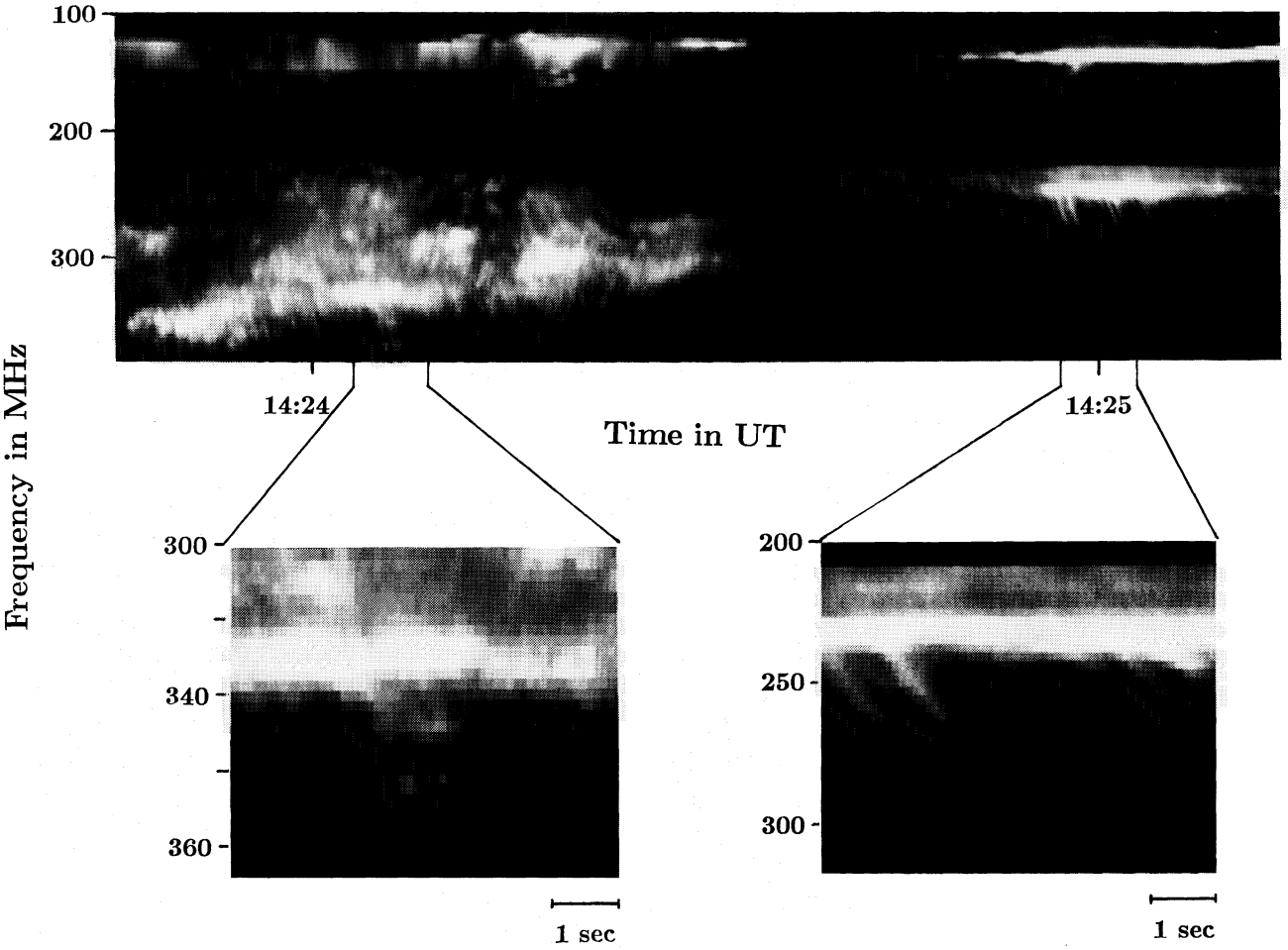

Fig. 1. *Top:* Spectrogramme of a section of a solar type II radio burst recorded with the IKARUS spectrometer at ETH Zürich on 1980 April 6. The brightness indicates radio flux in a logarithmic scale. *Bottom:* Two enlargements of the above overview showing horizontal "backbone" and vertical (skew) "herringbone" structures

and Melsose, 1985). This suggests emission in the ordinary mode also for the "backbone" component.

4) A very basic property is the frequent appearance of harmonic bands, although the fundamental may sometimes be missing in sources from near or behind the limb (Nelson and Melrose, 1985). It is important that not only the "herringbones" show harmonic structures (as do type III bursts), but even more frequently this is observed for the "backbone". It indicates a similarity of the emission mechanisms of the two components, which, in general terms, seems to require the presence of high-frequency turbulence and ion density fluctuations or low-frequency waves in both cases. We further note that harmonic structure is also observed in radio emission from interplanetary shocks (Lengyel et al., 1985; Cane et al., 1982) and the Earth's bow shock (Hoang et al., 1981, and references therein).

A rich collection of observations on the Earth's bow shock has been gathered by the ISEE and other spacecraft throughout the 1970's and early 80's. Extensive reports have been published in a special issue of the *J. Geophys. Res.* **86**, 4319–4536 (1981), and Russel and Hoppe (1983) have reviewed the results. It is clear now that a significant amount (about 1%) of the solar wind energy is converted into suprathermal and energetic particles accelerated into the upstream region. There are four major constituents: (i) reflected protons forming field aligned beams of a few keV in the sunward direction, (ii) diffuse protons with broad energy and angular distributions, which may (at least partially) originate from the beam by quasi-linear diffusion, (iii) electron beams of 1–2 keV energy particles observed mainly on interplanetary magnetic field lines which are newly connected to the bow shock, and (iv) a suprathermal electron tail (<1 keV) in the sunward direction. Electrons and protons with energies >100 keV have also been reported. Energetically, they are however unimportant.

An overview on the major upstream waves at the Earth's bow shock has been presented by Anderson et al. (1981) and Tsurutani and Rodriguez (1981). In particular note strong magneto-acoustic and Whistler waves generally associated with ion beams, and field aligned Langmuir waves at the local plasma frequency. The waves correlate with the electron beams (Scarf et al., 1971) and have phase velocities of $1–2\ 10^9$ cm s^{-1} corresponding to the observed electron energies of a few keV. These relatively slow beams are reminiscent of the herringbone structures of coronal type II bursts, which often have relatively small frequency drifts compared to flare initiated type III bursts generally associated with 20 keV electrons. With Holman and Pesses (1983), Krasnosel'skikh et al. (1985), Thejappa (1986) and others we conclude that the herringbone type of emission is caused by this species of low energy electron beams.

In addition, ion-acoustic waves of unknown origin are frequently observed in regions upstream of parallel shocks, and other, even lower frequency, unidentified electrostatic emissions

have been reported by Anderson et al. (1981). Vaisberg et al. (1983), and Galeev et al. (1986) have possibly identified lower-hybrid waves.

The IMP-6 and ISEE-3 spacecraft have also observed the radio emission of the bow shock (Hoang et al., 1981, and references therein). The bandwidth of the harmonic is extremely narrow (sometimes less than 3% of the center frequency) and is apparently caused by inhomogeneity in the upstream solar wind. The fundamental and harmonic bands resemble the "backbone" emission of coronal shocks. A warning against rapid conclusions may be appropriate: "Herringbone" structure would be expected to drift very slowly due to the density scale height of the solar wind being about three orders of magnitude larger than in the corona. It would not have been distinguished by the spectrometers of these experiments from "backbone" emission. Assuming unpolarized emission Hoang et al. observed the harmonic emission from a point source ($\ll 10^6$ km size) displaced some 10–30 Earth radii (up to 60) from the subsolar point. However, if the emission is 100% linearly polarized, its centroid position agrees very suggestively with the subsolar point. It remains unclear whether the radio emission of the bow shock is the equivalent of the "herringbone", the "backbone", or both superposed.

Similar phenomena have been found in shocks travelling in interplanetary space. Not every shock, however, has all the bow shock features (Kennel et al., 1982). In fact, the bow shock comprises quasi-perpendicular as well as quasi-parallel sections, on the other hand interplanetary shocks may have smaller curvature with less variation in shock angle. Generally, the particle fluxes are less intense but extend to higher energies. This may be explained by the lower Mach number, but greater spatial extent of interplanetary shocks.

Coronal shocks are expected to be even more different (e.g. due to the relatively stronger magnetic field). We note *en passant* that just the power emitted in radio waves of the coronal type II backbone (about 5 10^{18} erg/s) exceeds the energy flux of all upstream particles from the Earth's bow shock (10^{17}–10^{18} erg s^{-1}). In addition to the established properties of coronal type II events and collisionless shocks we make the following assumptions for which there is observational evidence, but yet no proof:

1) The velocity of shocks causing type II bursts is *supercritical*, i.e. their Mach number exceeds a threshold (between about 1.1 and 2.2 depending on the upstream plasma parameters) as suggested by Thejappa (1987). At the critical Mach number an ion acoustic subshock develops on which potential a considerable fraction of ions is reflected and energized. Bavassano et al. (1986) have shown that most interplanetary shocks are supercritical and consequently show signature of ion reflection, such as magnetic overshoots and "feet" of magnetic turbulence in the upstream region. The assumption is compatible with the observation of Gosling et al. (1976) that the rate of type II burst association of coronal mass ejections (CME) observed in white light increases with their speed. However, Kahler et al. (1985) concluded that $33 \pm 15\%$ of all fast (> 500 km/s) CME's had no associated coronal type II burst, confirming an earlier observation by Sheeley et al. (1984) of major visible-disk flares with fast CME, large interplanetary shocks but no obvious coronal type II burst. There seems to be at least one more condition for radio emission of shocks.

2) This additional condition may be that the radio emitting shocks must have a region of *quasi-perpendicular propagation*. Obviously, one expects that the prevalent motion of a type II producing shock is radial, thus mostly parallel to the magnetic field at least in the higher corona. Nevertheless, a considerable transverse expansion and substantial deviations from a strictly radial may occur. We make this assumption mainly in analogy to the bow shock, where the point of tangency of shock surface and solar wind magnetic field is the well known site of efficient electron acceleration. There is some support of this assumption from the observation of Stewart and Magun (1980) of horizontal source motions of herringbones transverse to the direction of the shock.

3) Finally, we consider a type II source in the upstream region in agreement with interplanetary shocks. It is also compatible with observations of Hoang et al. (1981) of the second harmonic radio emission of the bow shock to be at twice the local plasma frequency of the upstream solar wind. The situation is less clear for coronal type II sources. Wagner and McQueen (1983) and Gary et al. (1984) have found the position of a coronal type II source below the associated CME, a loop transient observed by the white light coronograph on board the SMM spacecraft. Since there is no support for propagating energetic electrons or connecting field lines into the region far downstream, they propose a second shock, possibly a blast wave, to be the origin of the type II burst. Coronal observations do not exclude our assumption of an upstream radio source for coronal type II bursts.

Excluding type III-like theories for the emission process of the backbone radiation, we are left with few alternatives. A possibility may be a cloud of energetic electrons co-moving with the shock preferably having a "gap" distribution in velocity (isotropic with an enhanced shell of some suprathermal speed). However, Nelson and Melrose (1985) have argued that the resulting maximum brightness temperature would be far below the observed values. A second possibility, maser emission, has recently been proposed by Wu et al. (1986). Since the ratio of electron gyrofrequency to plasma frequency is much smaller than unity, they find the electromagnetic electron cyclotron instability to simultaneously occur at several high harmonics of the gyrofrequency. Their direct emission process seems to be very attractive from the point of view of radiation theory. However, they cannot explain the ubiquitous fundamental/second harmonic structures in the radio emission of coronal, interplanetary and bow shocks. They are often observed to be close to a factor 2 in frequency (e.g. Weiss, 1965; Lengyel et al., 1985, and others). Also, it remains unclear why "backbone" patches often are extremely narrowbanded and their frequency and polarization are so similar to the type III-like "herringbones". For these reasons we propose here an alternative to their model and suggest further observational tests.

2. Electrons

Non-thermal electrons are an essential ingredient of all models for type II emission. Energetic electrons are ubiquitous in the upstream of the Earth's bow shock. They propagate in the sunward direction along interplanetary magnetic field lines connecting to near the point of tangency where the shock propagation is perpendicular to the field (Fan et al., 1964; Anderson, 1968; Ogilvie et al., 1971; Feldman et al., 1973; Anderson et al., 1979 and many others, cf. Fig. 2). The problem of acceleration of these electrons is still a matter of ongoing research. There are two major lines of work. The first approach invokes resonant diffusion in the low-frequency turbulence driven by the ion beams. The main features have been proposed by Papadopoulos (1981), later developed by Vaisberg et al. (1983), and applied to solar type II radio bursts by Krasnosel'skikh et al. (1985) and Thejappa (1987). It is based on the idea that the reflected ions near the point of tangency form a beam perpendicular to the magnetic field. As will

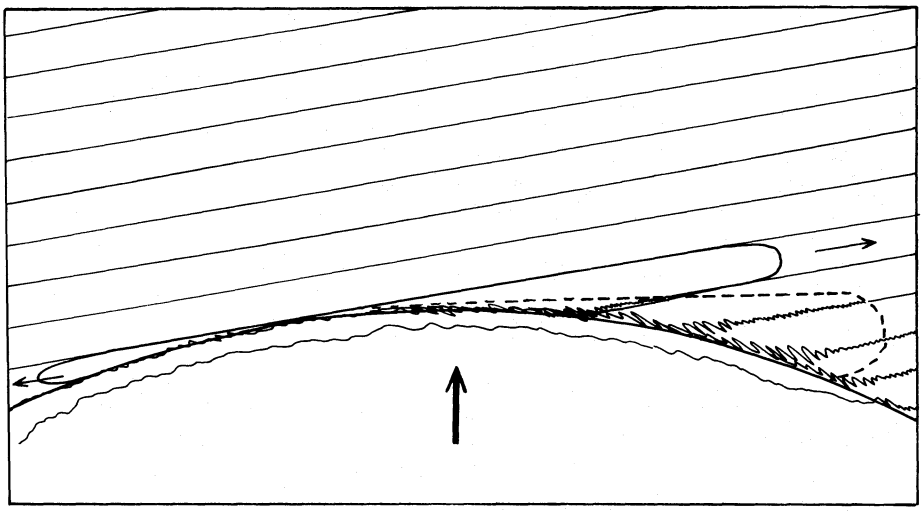

Fig. 2. Schematic overview on coronal shock structure. The shock front (*heavy curve*) moves up in the picture (*heavy arrow*). The magnetic field (*thin lines and curves*) is compressed in the shock. Electrons are accelerated into the upstream region (*thin arrows*) and are confined to the electron foreshock below the tangential field line. Their distribution may be unstable towards growing upper-hybrid waves in the upper lobe (*full curve*). Accelerated ions are unstable to magnetosonic waves (*represented by wiggles in the magnetic field*) which form the "foot" of the shock. They also may cause growing lower-hybrid waves in the lower lobe (*dashed curve*) in the ion foreshock

be shown in the next section, such an ion beam drives low-frequency waves unstable ($\Omega_i \ll \omega \ll \Omega_e$) with $k_\perp \gg k_\parallel$. Since the phase velocities of these waves along the magnetic field lines are very high, the magnetized background electrons absorb these waves by Cherenkov resonance, $\omega = k_\parallel v_\parallel$, and get stochastically accelerated. As a result the non-Maxwellian tail of the electron distribution grows.

Here we will consider a second mechanism, often referred to as Fast Fermi Acceleration. It is mainly based on adiabatic reflection of incident electrons in the de Hoffman-Teller (HT) frame of reference, which is defined such that the upstream velocity as seen in this frame is aligned with the upstream magnetic field. The electric field of the upstream motion, $-\frac{1}{c}\boldsymbol{V}\times\boldsymbol{B}$, therefore vanishes. Electrons are reflected mainly by the rise in the magnetic field strength at the shock combined with a jump of the electric potential. The average energy per reflected electron scales as $\approx(\frac{1}{2}m V_0^2)\,4/\cos^2\Theta_{Bn}$ for large Θ_{Bn}, the angle between upstream magnetic field and shock normal, V_0 is the upstream flow velocity (or shock speed). The energization is appreciable as this angle is close to perpendicular.

The above mechanism is based on the acceleration process proposed by Fermi (1949) for cosmic rays. Feldman et al. (1983) described how the shock can behave like a magnetic mirror. Leroy and Mangeney (1984) and Wu (1984) worked out the case of adiabatic reflection (gyroradius ≪ shock thickness) for essentially thermal or moderately suprathermal upstream electrons. They have shown that the velocity distribution of the reflected electrons is a shifted loss-cone. Inserting for the potential and integrating over perpendicular velocity, $u_\perp$,in the HT frame, the distribution function of the reflected electrons becomes

$$F_r(u_\parallel) = n_e\left(\frac{m}{2\pi T_e}\right)^{1/2} \exp\left(-\frac{B_0}{B_1-B_0}\frac{e\phi'}{T_e} - \frac{m}{2T_e}\frac{B_0}{B_1}U_0^2\right) \cdot \exp\left[-\frac{m}{2T_e}\frac{B_1}{B_1-B_0}\left(u_\parallel + U_0\left(\frac{B_1-B_0}{B_1}\right)\right)^2\right] \quad (1)$$

(Leroy and Mangeney, 1984). Here the upstream electron distribution is considered a Maxwellian with temperature T_e (in units of energy). B_0 and B_1 are the magnetic field strengths in the upstream and the shock front, respectively, and ϕ' is the electric potential in the HT frame. The parameters for coronal type II emitting shocks will typically be $B_1/B_0 \approx 3$, and $e\phi'/T_e \approx 1$. The particle velocity parallel to the magnetic field, $u_\parallel$, and the upstream velocity, U_0, both measured in the HT frame can be expressed as

$$u_\parallel = v_\parallel = \boldsymbol{V}_{\mathrm{HT}} \cdot \boldsymbol{b}, \quad (2)$$

$$\boldsymbol{U}_0 = V_0 \frac{\cos\Theta_{vn}}{\cos\Theta_{Bn}}\boldsymbol{b}, \quad (3)$$

where V_{HT} is the velocity of the HT frame with respect to the observer's frame, $\boldsymbol{b}$ is the unit vector along the magnetic field, and Θ_{vn} the angle between upstream velocity and shock normal. We approximate the electron distribution function (1) by a displaced ring

$$F_r(\boldsymbol{u}) = A \exp\left[-\frac{(u_\parallel - U_{0\parallel})^2}{2\alpha_\parallel^2} - \frac{(u_\perp - U_{0\perp})^2}{2\alpha_\perp^2}\right], \quad (4)$$

where the normalization, $\int F_r\, d^3u = 1$, requires

$$A = \left[\pi^{3/2}\alpha_\perp^2\alpha_\parallel\left\{\exp\left(-\frac{U_{0\perp}^2}{u_\perp^2}\right) + \pi^{1/2}\frac{U_{0\perp}^2}{\alpha_\perp}\left[1+\mathrm{erf}\left(\frac{U_{0\perp}}{\alpha_\perp}\right)\right]\right\}\right]^{-1}. \quad (5)$$

Which instabilities will be driven by this distribution? For $\Omega_e^2/\omega_{pe}^2 \ll 1$ it unfortunately depends very much on details. We may distinguish two groups of instabilities: those acting mainly on the positive gradient in $u_\parallel$ reducing the shift $U_{0\parallel}$, and others that are mainly driven by the perpendicular gradient eroding the ring. The former have been investigated in connection with the type III process. Field aligned, electrostatic oscillations above the plasma frequency (Langmuir waves) are well known and observed to grow in such circumstances. As solar type III radio bursts show, electron beams with positive gradients can exist for several minutes due to quenching of the instability by density inhomogeneities, reabsorption of the waves, and spatial diffusion. Such a stabilized beam may well be the exciter of "herringbone" structure in type II bursts, but not the source of the quasi-stationary "backbone" (cf. Sect. 1).

Less is known about the instabilities of the ring component of distribution (4). Anisotropies in velocity space with enhanced perpendicular energy lead to whistler instability over a wide range of parameters. Among the electrostatic ring or loss-cone instabilities the upper-hybrid mode grows fastest. This wave is the generalized Langmuir mode propagating perpendicular to the field and is equivalent to the Z-mode in our limit $\omega_p \gg \Omega_e$. The two

instabilities have been compared for $\omega_p^2 \gg \Omega_e^2$ by Berney and Benz (1978) and Sharma and Vlahos (1984) for special cases of the upper-hybrid mode. A more general treatment of the latter was given by Winglee and Dulk (1986), who used the full "maser" approach and found even larger growth rates particularly at places where the local plasma frequency is about an integer multiple of the electron gyrofrequency. Whistler waves are driven by the general anisotropy of the ring distribution, but upper hybrid waves grow on the positive slope of $f(v_\perp)$. The most unstable modes of the two waves are in resonance with different particles. Whistlers interact more with energetic particles, lower-hybrid waves with ring electrons having small $v_\perp$. Upper-hybrid waves are generally more unstable compared to whistlers for large ratios ω_p/Ω_e and small fractions of energetic particles (Berney and Benz, 1978). Thus we can expect that electrons accelerated by the fast Fermi process drive upper-hybrid waves unstable.

The dispersion relation for the high frequency electrostatic oscillations of a cold plasma is

$$\varepsilon_0 = 1 - \frac{\omega_{pe}^2}{\omega^2}\left(\frac{k_\parallel}{k}\right)^2 - \frac{\omega_{pe}^2}{\omega^2 - \Omega_e^2}\left(\frac{k_\perp}{k}\right)^2 = 0 \tag{6}$$

For $k_\parallel \ll k$ and $\Omega_e^2 \ll \omega_{pe}^2$ the solution of Eq. (6) is

$$\omega = \omega_{pe} + \frac{1}{2}\frac{\Omega_e^2}{\omega_{pe}^2}\left(\frac{k_\perp}{k}\right)^2 \tag{7}$$

Adding a small population ($n_E \ll n_0$) of energetic electrons, but neglecting its contribution to the real part of ε_0, the linear growth rate of the waves growing at ω is given by

$$\frac{\gamma}{\omega} \approx \frac{\pi}{2}\frac{n_E}{n_0}\frac{\omega_{pe}^2}{\omega^2}\sum_s \int d^3v J_s^2\left(\frac{k_\perp u_\perp}{\Omega_e}\right)s^2\Omega_e^2 \cdot \left(\frac{s\Omega_e}{u_\perp}\frac{\partial f}{\partial u_\perp} + k_\parallel \frac{\partial f}{\partial u_\parallel}\right)\cdot \delta\left(\omega - \frac{k_\parallel u_\parallel}{\gamma} - \frac{s\Omega_e}{\gamma}\right), \tag{8}$$

where J_s is the Bessel function of the first kind of order s.

We do not know how these waves saturate. Pritchett (1986) has convincingly shown that for $\omega_p \ll \Omega_e$ and X-mode the maser instability saturates by quasilinear diffusion. Another possibility is electron trapping (Le Quéan et al., 1984). Benz (1980) assuming saturation by the non-linear shift of the gyrofrequency arrives at a wave energy level (relative to nT_e) of

$$\beta_{uh} \approx \frac{\alpha}{32\, s^2\left(1 - \frac{9\alpha}{2}\right)}\frac{n_E}{n_0}\left(\frac{\alpha_\perp}{v_e}\right)^2 \tag{9}$$

for a special case (hydrodynamic approach), and where $v_e^2 = T_e/m_e$ refers to the cold background electrons, $\alpha \equiv (s/k\,R_e)^2$, $s \equiv \omega_p/\Omega_e$, and $R_e \equiv v_e/\Omega_e$. We will use $s = 10$ and $\alpha = 0.15$. Leroy and Mangeney (1984) have evaluated the energy and density of the reflected electrons from the shock front at various angles Θ_{Bn}. A rough estimate of the energy density in upper-hybrid waves is given in Table 1 using Eq. (9). The number of reflected electrons and the energy density of the waves increase with smaller Θ_{Bn}. The kinetic energy of the accelerated particles, however, decrease to $4.1\,KT_e$ at 83°. Below this angle the energy rapidly falls below $2\,KT_e$, the approximate limit of instability.

Table 1. Fraction of energetic electrons accelerated at various shock angles Θ_{Bn} (Leroy and Mangeney, 1984), perpendicular temperature of reflected electrons, and approximate level of upper-hybrid waves β_{uh} [in units of $n_0\,T_e$ after Eq. (9)]

Θ_{Bn}	n_E/n_0	$T_\perp/T_e$	β_{uh}
83°	$1.1\ 10^{-1}$	3.0	$4.6\ 10^{-5}$
86°	$6.0\ 10^{-2}$	3.5	$2.9\ 10^{-5}$
88°	$2.9\ 10^{-3}$	5.8	$2.4\ 10^{-6}$
88°5	$1.3\ 10^{-4}$	8.3	$1.5\ 10^{-7}$
89°	$1.7\ 10^{-8}$	15.0	$3.6\ 10^{-11}$
89°5	$1.0\ 10^{-29}$	51.0	$7.1\ 10^{-32}$

3. Ions

Ions may take up a considerably larger fraction of the shock energy than electrons. Energetic ions and their wave turbulence have important feedback effects on the shock and should not be neglected in a model for type II burst emission. Ions with energies small in comparison with the potential barrier in the shock front cannot pass and get reflected into the upstream. The theoretical analysis of quasi-perpendicular shocks shows that when the Alfvènic Mach number exceeds some critical value $M_c = V_0/v_A \approx 2$, the potential is equal to the energy of the ions in the upstream and reflects an important fraction of the ions (Sagdeev, 1964; Biskamp, 1973; Tidman and Krall, 1971; Leroy et al., 1981, 1982).

The reflected ions cause very low frequency magnetosonic turbulence giving rise to a "foot" structure in the magnetic field ahead of the main shock. The thickness of the "foot" is of the order of V_0/Ω_i. In this region a small preliminary deceleration of the upstream plasma and increase in density and magnetic field take place. These theoretical conclusions are well supported by in situ observations near the Earth's bow shock (cf. review by Russel and Hoppe, 1983) and by numerical simulations of collisionless shocks (Chodura, 1975; Leroy et al., 1981, 1982).

These ions form a beam with velocity $v_b \approx 2\,V_0$ in the frame of reference moving with the plasma stream. The beam density, n_b, is approximately $(0.1\text{–}0.3)\,n_0$ (Leroy et al., 1981, 1982; Krasnosel'skikh et al., 1985). A drifting Maxwellian approximately describes the ion beam

$$f_b(\boldsymbol{v}) = \left(\frac{1}{\pi v_{Tb}}\right)^{3/2} \exp\left[-(\boldsymbol{v} - \boldsymbol{v}_b)^2/v_{Tb}^2\right], \tag{10}$$

where v_{Tb} is the thermal spread in the ion beam.

Here we are mostly interested in waves that can coalesce with high-frequency waves (discussed in Sect. 2) to radiate fundamental plasma emission. The wave vektor $\boldsymbol{k}$ of such a mode must satisfy the coupling condition $\boldsymbol{k}_{uh} + \boldsymbol{k} = \boldsymbol{k}_r$, where the radio wave $\boldsymbol{k}$-vector, $\boldsymbol{k}_r$, is relatively short. Therefore a wave with large $\boldsymbol{k}$ perpendicular to the magnetic field is strongly favored.

A possible mode is the lower-hybrid wave which can interact with an ion beam and propagate almost perpendicular to the ambient field, if $n_b/n_0 \ll 1$ and $v_{Tb} \ll v_b$. Our choice of the type of low-frequency waves is not unique. We note, however, that electron and ion temperatures in the corona are expected to be similar. Therefore, the energy density in ion-acoustic waves is likely to be far below the levels observed in the solar wind and near the bow shock. Since lower-hybrid waves exist independently of the ratio T_e/T_i, their role could be important in stellar atmospheres. For the usual coronal assumptions, $\Omega_e \ll \omega_p$, $\beta_{e,i} \equiv 8\pi n T_{e,i}/B^2 \ll 1$, the general dispersion relation for

electrostatic waves propagating almost perpendicular to the magnetic field is

$$\varepsilon_0 = 1 + \frac{\omega_{pe}^2}{\Omega_e^2}\left(\frac{k_\perp}{k}\right)^2 - \frac{\omega_{pe}^2}{\omega^2}\left(\frac{k_\parallel}{k}\right)^2 - \frac{\omega_{pi}^2}{\omega^2} = 0, \tag{11}$$

where the approximation $k_\parallel^2 \ll k_\perp^2$ has been made in the dielectric response of the background ions. The contribution of the reflected ions to the real part of the dielectric constant, ε_0, is neglected. The solution of Eq. (4) for $\Omega_e \gg \omega \gg \Omega_i$ and $\mathrm{Im}\,\omega \gg \Omega_i$ is then

$$\omega^2 \approx \omega_{lh}^2\left[1 + \frac{m_i}{m_e}\left(\frac{k_\parallel}{k}\right)^2 + \left(\frac{3}{4} + \frac{3\,T_i}{T_e}\right) k^2 R_e^2\right], \tag{12}$$

where we have added the thermal effects in the last term in the bracket, and used the definition $\omega_{lh}^2 \equiv \Omega_e \Omega_i$. The derivative of ε_0 with respect to ω can easily be evaluated

$$\omega \frac{\partial \varepsilon_0}{\partial \omega} = 2\frac{\omega_{pe}^2}{\Omega_e^2}. \tag{13}$$

The contribution of the beam distribution (10) to the longitudinal dielectric permittivity is

$$\varepsilon_b = \frac{n_b}{n_0}\frac{\omega_{pi}^2}{k^2}\int \frac{\boldsymbol{k}\partial f_b/\partial \boldsymbol{v}}{\omega - \boldsymbol{k}\boldsymbol{v}}\, d^3 v. \tag{14}$$

Its imaginary part for $k_\perp R_i \gg 1 \gg k_\perp R_e$ i.e. for strongly magnetized electrons and unmagnetized ions has been derived by Krasnosel'skikh et al. (1985):

$$\mathrm{Im}\,\varepsilon_b = 2\pi \frac{n_b}{n_0}\frac{\omega_{pi}^2}{k^2 v_{tb}^2}\frac{(\boldsymbol{k}\boldsymbol{v}_b - \omega)}{k\, v_{tb}} \exp\left[-\frac{(\boldsymbol{k}\,\boldsymbol{v}_b - \omega)^2}{k^2 v_{tb}^2}\right]. \tag{15}$$

The term $(\boldsymbol{k}\,\boldsymbol{v}_b - \omega)/k\,v_{tb}$ is of order unity. Thus the growth rate of the lower-hybrid waves excited by the reflected ions can be evaluated in the conventional way

$$\gamma_{lh} = -\frac{\mathrm{Im}\,\varepsilon_b}{\partial \varepsilon_0/\partial \omega|_{\varepsilon_0 = 0}} \tag{16}$$

for $\gamma_{lh} \ll \omega$, leading to

$$\frac{\gamma_{lh}}{\omega} \approx \pi e^{-1}\frac{\omega_{lh}^2}{(k\,v_{Tb})^2}\frac{n_b}{n_0}. \tag{17}$$

McBride et al. (1972) have shown that wave growth cannot continue after ion trapping, which occurs when the wave energy density, β_{lh}, in units of nT_e, reaches

$$\beta_{lh} \approx 0.05\left(1 + \frac{\omega_{pe}^2}{\Omega_e^2}\right)^{-1}. \tag{18}$$

4. Radio emission

In this section we consider the nonlinear interaction of the electrostatic waves driven unstable by electrons and ions accelerated at the shock. Note that the waves do not necessarily coincide in space. An overview is given in Fig. 2. Upper-hybrid waves may be excited by the loss-one distribution of electrons accelerated by the fast Fermi mechanism. Thus the waves are limited to a small region near the shock in the electron foreshock. Ion waves are excited by reflected ions in the ion foreshock, the front of which lags behind due to the slower motions of accelerated ions.

It is very likely that these electrostatic waves interact between themselves and, in regions of overlapping turbulence, on each other and get converted into electromagnetic radiation. Then, if subscripts 1 and 2 refer to the primary electrostatic waves, and subscript 3 stands for the electromagnetic wave, the following coupling conditions should be satisfied:

$$\boldsymbol{k}_3 = \boldsymbol{k}_1 \pm \boldsymbol{k}_2, \tag{19}$$

$$\omega_3 = \omega_1 \pm \omega_2, \tag{20}$$

$$D(\omega_i, \boldsymbol{k}_i) = 0, \tag{21}$$

where D is the dispersion relation and $i = 1, 2, 3$. Since the electrostatic waves discussed in the two previous sections all have phase velocities $\ll c$, their $\boldsymbol{k}$-vectors are relatively large. Thus

$$|\boldsymbol{k}_3| \approx \frac{\omega}{c} \ll |\boldsymbol{k}_{1,2}| \tag{22}$$

Equation (19) can then only be satisfied if the primary waves are nearly oppositely directed. Near the upper-hybrid and lower-hybrid resonances $|\boldsymbol{k}_{\parallel 1}|$ and $|\boldsymbol{k}_{\parallel 2}|$ are very small, thus $|\boldsymbol{k}_{\perp 1}| \approx |\boldsymbol{k}_{\perp 2}|$. Waves with anisotropic $\boldsymbol{k}$ distributions such as waves with $\omega \approx \omega_{uh}$ or ω_{lh} are well suited to produce the very high brightness temperature observed in type II radio bursts by the three wave process. There are two possible cases: 1) $\omega_1 \approx \omega_2 \approx \omega_{uh}$ in the electron foreshock and 2) $\omega_1 \approx \omega_{uh}$ and $\omega_2 \approx \omega_{lh}$ in the overlap of electron and ion foreshock (cf. Fig. 2). The resulting frequencies of the resulting electromagnetic radiation are $\omega_3 \approx 2\omega_{uh}$ and $\omega_3 \approx \omega_{uh}$, respectively.

4.1. Radiation at the fundamental

In principle, the coupling at the fundamental, $\omega_{lh} + \omega_{uh}$, can be either O-mode or X-mode. Since X-mode at ω_{uh} cannot escape from the source region, only O-mode is of our interest. The parallel components of the $\boldsymbol{k}$-vectors of the electrostatic waves are very small, and they couple preferentially to nearly perpendicular transverse waves. Note that O-mode waves propagating perpendicular to the magnetic field (as observed at the bow shock from ISEE-3) are linearly polarized parallel to $\boldsymbol{B}_0$. As soon as they leave the quasi-transverse region, however, the waves Faraday rotate to nearly vanishing circular polarization as observed.

Furthermore, the interaction takes place in the "foot" of the shock at enhanced densities. The radiation can thus easily escape and will appear at a slightly enhanced frequency in relation to the undisturbed corona.

The electrostatic waves having $\omega \approx \omega_{lh}$ and $\omega \approx \omega_{uh}$ are expected to have large amplitudes, and (if linear) they have rather narrow spectra and emission angles. Since the energy density of low-frequency waves [Eq. (18)] far exceeds that of the high-frequency waves (Table 1), the opacity, μ, is due to the lower-hybrid waves. For coronal conditions (Wentzel, 1981)

$$\mu_{lh} \approx 0.1\,\beta_{lh} \quad \mathrm{cm}^{-1}. \tag{23}$$

High- and low-frequency waves need to interact only a very short distance to reach high optical depth. For $\omega_p = 10\,\Omega_e$ and using Eq. (18) optical thickness unity can be accomplished over $2\ 10^4$ cm. The radio brightness temperature, T_r, then equals the temperature of the waves with lower quantum density N defined as

$$T_{uh} \equiv \hbar\omega_{uh} N_{uh} = \frac{(2\pi)^3 \beta_{uh} n T_e}{\Omega k_{uh}^2 \Delta k_{uh}}, \tag{24}$$

where Ω is the wave solid angle and Δk_{uh} the spectral range of the upper-hybrid waves. In our case typically

$$T_{uh} \approx 10^{18} \cdot \frac{\beta_{uh}}{\Omega}\,\mathrm{K}. \tag{25}$$

For $\Omega = 4\pi k_{\parallel}/k = 4\pi \sqrt{m_e/m_i} \approx 0.3$ sterad and $\Theta_{Bn} \approx 83°$ this leads to a radio brightness temperature at the fundamental

$$T_{rf} = T_{uh} \approx 1.5\ 10^{14}\,\mathrm{K}\,, \tag{26}$$

compatible with observation.

4.2. *Radiation at the harmonic*

Radiation at about $2\omega_{uh}$ can be emitted from the region of upper-hybrid instability in the electron foreshock (cf. Fig. 2). The coalescence process is very effective since the waves fill only a small solid angle near the perpendicular plane. For coronal conditions the absorption coefficient of this mechanism is (e.g. Smith and Spicer, 1979)

$$\mu_{uh} \approx 2\ 10^{-4}\,\beta_{uh}\,\mathrm{cm}^{-1}\,. \tag{27}$$

With the estimated values of Table 1 and the source dimensions derived from observations it is clear that the harmonic radiation is marginally (but not always) optically thick. The maximum brightness temperature of the harmonic is again T_{uh} (cf. Eq. 24) and

$$T_{rh} \leqq T_{uh}\,. \tag{28}$$

Again the transverse waves are preferentially emitted perpendicular to $\boldsymbol{B}$. Their initial linear polarization is smeared out by Faraday rotation. Thus the observed net circular polarization nearly vanishes.

5. Discussion

A self-consistent theory of radio emission by coronal shocks has been developed to explain the narrowband, non-streaming source of the "backbone" of type II bursts. The starting point are some basic, well accepted observational facts on the radio emission as well as particle and wave measurements at the Earth's bow shock and on interplanetary shocks. The emission is proposed to be the result of the coupling between high and low-frequency plasma waves. The relevant wave modes have been selected in view of the observed properties, but need confirmation by further observations.

The high-frequency waves are identified with the upper-hybrid mode predicted by the ring distribution resulting from fast Fermi electron acceleration. The waves reach maximum saturation level at places of quasi-perpendicular shock propagation (83° for the parameters used by Leroy and Mangeney, 1984), since the number of accelerated electrons decreases towards 90° and their energy falls below the instability threshold for angles smaller than 83°. The parallel size, $s_{\parallel}$, of the region of turbulence corresponds to a range of changes of shock angles Θ_{Bn}. It is $s_{\parallel} \approx r \sin \Delta\Theta_{Bn} \cdot \cos\Theta_{Bn} \approx 1000\,\mathrm{km}$ where the shock radius of curvature, r, was taken to be 10^{11} cm, and the halfpower width $\Delta\Theta_{Bn} \approx 0.^{\circ}5$ (cf. Table 1). The size perpendicular to the upstream magnetic field is given by $s_{\perp} \approx s_{\parallel}\, v_{\perp}/v_{\parallel}$. If we take the velocity of the accelerated electrons $v_{\parallel} \approx c/10$, resp. $v_{\perp} \approx c/50$, we get the perpendicular size, $s_{\perp} \approx 200\,\mathrm{km}$. Thus the source dimensions are well within the limits set by observations. For the Earth's bow shock this model also predicts nearly perpendicular upper-hybrid waves in a volume smaller in size by about an order of magnitude, due to the smaller radius of shock curvature. Such waves have not yet been discovered.

Whereas the source size of harmonic radiation is identical to the region of enhanced upper-hybrid turbulence, fundamental emission is strongly enhanced in the part of the region overlapping with low-frequency turbulence. Thus the source of the fundamental emission (before scattering during propagation) may be even smaller. This agrees with observations by Lengyel et al. (1985) of a smaller bandwidth to frequency ratio of the fundamental (indicating a more homogeneous or smaller source). The frequent observation of simultaneous turn-on of fundamental and harmonic bands in type II bursts suggests that the start of radio emission of coronal shocks is determined by electron acceleration. Since the conditions of fast Fermi acceleration are supersonic disturbance and quasi-perpendicular propagation, the on-set of radio emission (as well as its end) is an interesting point in the evolution of coronal shocks. We have related theory to observations already with the assumptions on bandwidth, upstream location, fundamental/harmonic structure and the presence of energetic particles as manifested in "herringbone". In addition the model can explain several other observational facts:

1. Preferential emission in transverse direction leads to low polarization by Faraday rotation in agreement with a very characteristic property of type II bursts.

2. The brightness temperatures derived in Eqs. (26) and (28) imply that the fundamental and harmonic "backbone" emissions may have the same flux. This is in fact observed for a part of the type II bursts. The differences in source size, free-free absorption and/or scattering in the corona can be drastic, however, and may be responsible for the others.

3. The model predicts radio emission for all supercritical, quasi-perpendicular shocks. Since the shock angle can be close to 90° in several regions of the shock surface, this may explain multiple sources and tangential source motions.

Future work will have to show the existence of perpendicular electrostatic waves both at high and low frequency in the bow shock or interplanetary shocks. Theoretical studies are needed of the threshold, evolution, and saturation of instabilities of loss-cone-type velocity distributions at large ratios of ω_p/Ω_e. High resolution radio spectrogrammes may better reveal the detailed relation of "backbone" emission and "herringbones" suggested in Fig. 1. Other fine structures, such as bandsplitting, requires further theoretical and observational scrutiny. Polarigrammes are of particular interest to show the differences in emission mode. With the upcoming possibilities of EUV coronal observation, the predicted coincidence of "backbone" source position and points of tangency of the shock surface and magnetic field will be subject to direct tests. The phase of radio emission seems to be an interesting part of coronal shocks directly related to its capability of electron (and to a lesser extent) proton acceleration.

Acknowledgements. The construction of the ETH radio spectrometers is partially supported by the Swiss National Science Foundation (grant No. 2.019-0.86).

References

Anderson, K.A.: 1968, *J. Geophys. Res.* **73**, 2387
Anderson, K.A., Lin, R.P., Martel, F., Lin, C.S., Parks, G.K., Reine, H.: *Geophys. Res. Letters* **6**, 401
Anderson, R.R., Parks, G.K., Eastman, T.E., Gurnett, D.A., Frank, L.A.: 1981, *J. Geophys. Res.* **86**, 4493
Bavassano-Cattaneo, M.B., Tsurutani, B.T., Smith, E.J.: 1986, *J. Geophys. Res.* **91**, 11929

Benz, A.O.: 1980, *Astrophys. J.* **240**, 892
Berney, M., Benz, A.O.: 1978, *Astron. Astrophys.* **65**, 369
Biskamp, D.: 1973, *Nuclear Fusion* **13**, 719
Cane, H.V., Stone, R.G., Fainberg, J., Steinberg, J.L., Hoang, S.: 1982, *Solar Phys.* **78**, 187
Chodura, R.: 1975, *Nuclear Fusion* **15**, 55
Fan, C.Y., Gloeckler, G., Simpson, J.A.: 1964, *Phys. Rev. Letters* **13**, 149
Feldman, W.C., Asbridge, J.R., Barne, S.J., Montgomery, M.D.: 1973, *J. Geophys.. Res.* **78**, 3697
Feldman, W.C., Anderson, R.C., Bame, S.J., Gary, S.P., Gary, S.P., Gosling, J.T. et al.: 1983, *J. Geophys. Res.* **88**, 96
Fermi, E.: 1949, *Phys. Rev.* **75**, 1149
Galeev, A.A., Klimov, S.I., Nogdrachev, M.N., Sagdeev, R.S., Sokolov, A.Y.: 1986, *Soviet Phys. JETP* **63**, 991
Gary, D.E., Dulk, G.A., House, L.L., Illing, R., Sawyer, C., Wagner, W.J., McLean, D.J., Hildner, E.: 1984, *Astron. Astrophys.* **134**, 222
Gosling, J.T., Hildner, E., MacQueen, R.M., Munro, R.H., Poland, A.F., Ross, C.L.: 1976, *Solar Phys.* **48**, 389
Hoang, S.J., Fainberg, J., Steinberg, J.L., Stone, R.G., Zwickl, R.H.: 1981, *J. Geophys. Res.* **86**, 4531
Holman, G.D., Pesses, M.E.: 1983, *Astrophys. J.* **267**, 837
Kahler, S.W., Reames, D.V., Sheeley, N.R.Jr., Howard, R.A., Koomen, M.J.: 1985, *Astrophys. J.* **290**, 742
Kennel, C.F., Scarf, F.L., Coroniti, F.V., Smith, E.J., Gurnett, D.A.: 1982, *J. Geophys. Res.* **87**, 17
Krasnosel'skikh, V.V., Kruchina, E.N., Thejappa, G., Volokitin, A.S.: 1985, *Astron. Astrophys.* **149**, 323
Lengyel-Frey, D., Stone, R.G., Bougeret, J.L.: 1985, *Astron. Astrophys.* **151**, 215
Le Quéau, D., Pellat, R., Roux, A.: 1984, *Phys. Fluids* **27**, 247
Leroy, M.M., Goodrich, C.C., Winske, D., Wu, C.S., Papadopoulos, K.: 1981, *Geophys. Res. Letters* **8**, 1268
Leroy, M.M., Goodrich, C.C., Winske, D., Wu, C.S., Papadopoulos, K.: 1982, *J. Geophys. Res.* **87**, 5081
Leroy, M.M., Mangeney, A.: 1984, *Ann. Geophys.* **2**, 449
McBride, J.B., Ott, E., Boris, J.P., Orens, J.H.: 1972, *Phys. Fluids* **15**, 2367
Nelson, G.J., Melrose, D.B.: 1985, *Solar Radiophys.* **333**
Ogilvie, K.W., Scudder, J.D., Sugiura, M.: 1971, *J. Geophys. Res.* **76**, 8165
Papadopoulos, K.: 1981, Proceedings of an International School and Workshop on Plasma Astrophysics held in Varenna, p. 313
Perrenoud, M.: 1982, *Solar Phys.* **81**, 197
Pritchett, P.L.: 1986, *Phys. Fluids* **29**, 2919
Roberts, J.A.: 1959, *Australian J. Phys.* **12**, 327
Russel, C.T., Hoppe, M.M.: 1983, *Space Sci. Rev.* **34**, 155
Sagdeev, R.Z.: 1964, Atomizdat, Problems of Plasma Theory **4**, 20
Scarf, F.L., Fredericks, R.W., Frank, L.A., Neugebauer, M.: 1971, *J. Geophys. Res.* **76**, 5162
Sharma, R.R., Vlahos, L.: 1984, *Astrophys. J.* **280**, 405
Sheeley, N.R., Stewart, R.T., Robinson, R.D., Howard, R.A., Koomen, M.J., Michels, D.J.: 1984, *Astrophys. J.* **279**, 839
Simnett, G.M.: 1986, *Solar Phys.* **104**, 67
Smith, D.F., Spicer, D.S.: 1979, *Solar Phys.* **62**, 359
Stewart, R.T., Magun, A.: 1980, *Proc. ASA* **4**, 53
Thejappa, G.: 1986, *Adv. Space Res.* **6**, 293
Thejappa, G.: 1987, *Solar Phys.* **111**, 45
Tidmann, D., Krall, N.: 1971, *Shock Waves in Collisionless Plasmas*, Wiley, New York
Tsurutani, B.T., Rodriguez, P.: 1981, *J. Geophys. Res.* **86**, 4319
Vaisberg, D.L. et al.: 1983, *Soviet Phys. JETP* **58**, 716
Wagner, W.J., MacQueen, R.M.: 1983, *Astron. Astrophys.* **120**, 136
Weiss, A.A.: 1965, *Australian J. Phys.* **18**, 167
Wentzel, D.G.: 1981, *Astron. Astrophys.* **100**, 20
Winglee, R.M., Dulk, G.A.: 1986, *Astrophys. J.* **307**, 808
Winglee, R.M., Dulk, G.A.: 1987, *Solar Phys.* **307**, 808
Wu, C.S.: 1984, *J. Geophys. Res.* **89**, 8857
Wu, C.S., Steinolfson, R.S., Zhon, G.C.: 1986, *Astrophys. J.* **309**, 392